

Large electromechanical response in ZnO and its microscopic origin

Dileep Karanth and Huaxiang Fu

Department of Physics, University of Arkansas, Fayetteville, Arkansas 72701, USA

(Received 13 May 2005; published 23 August 2005)

The electromechanical coefficient d_{33} of wurtzite ZnO is determined by direct first-principles density functional calculations which are performed for solids under finite electric fields. Our theoretical d_{33} value of 12.84 pC/N turns out to be in good agreement with experiment. This electromechanical response in ZnO (which is the largest among the known tetrahedral semiconductors) is found to originate from the strong coupling between strain and polarization, namely, a notably large β parameter. We further show that the electromechanical response in wurtzite semiconductors bears a previously unknown resemblance to the polarization rotation mechanism in ferroelectric Pb(ZnNb)O₃-PbTiO₃ and Pb(MgNb)O₃-PbTiO₃ single-crystal solid solutions. Our results demonstrate that, different from what is commonly believed, the main effect of electric fields in wurtzite semiconductors is not to elongate the polar chemical bonds, but to rotate those bonds that are non-collinear with the polar axis. This finding also suggests that the electromechanical response in wurtzite materials is governed mainly by the ease of bond bending, which may provide an useful scheme for designing better piezoelectric semiconductors with enhanced performance.

DOI: 10.1103/PhysRevB.72.064116

PACS number(s): 77.65.-j, 77.84.Bw

I. INTRODUCTION

Semiconductor ZnO is of growing technological importance due to its many favorable properties.¹ ZnO possesses large band gap (~ 3.44 eV) and high electric conductivity upon doping, often used as a candidate for transparent conducting oxides.² This material also shows strong bond strength, high melting temperature, large cohesive energy, and large exciton binding energy. The stability of ZnO is further ensured by its large shear modulus (~ 45 GPa). ZnO is thus more resistant to radiation and/or high temperature degradation, as compared to other semiconductors. Moreover, the drift mobility in ZnO saturates at higher fields and at higher values than most semiconductors, making it suitable for devices operating at high frequency.² The inexpensive availability of ZnO substrates is also an advantage.

Among the known tetrahedral semiconductors, ZnO has another distinctive property, that is, it exhibits the largest electromechanical response that is used in transducers of converting electrical energy into mechanical energy. Along with its preferable electronic properties as a semiconductor, ZnO is thus an interesting candidate for functioning as a multi-purpose material that combines superior electronic, optical, electrical, and piezoelectric properties. Another possible example of similar type of multipurpose semiconductor is the metastable ScN of a hexagonal structure as suggested in Ref. 3, but this material has an indirect band gap that is not appealing in optical applications. While the electronic properties of ZnO have now been rather well studied,⁴⁻⁶ its electromechanical properties are nevertheless poorly understood.^{7,8} Previously, Dal Corso *et al.* studied the piezoelectric constant e_{33} by computing the polarization response to applied strain *under zero field* and revealed that the clamped-ion contribution to the piezoelectric response cancels the internal atomic-relaxation contribution at the least degree in ZnO as compared to other semiconductors, thus giving rise to larger piezoelectric response.⁷ Hill and

Waghmare studied (also at zero electric field) the interplay between strain and electronic properties, showing that stress can be used to effectively tune the piezoelectric coefficient e_{33} .⁸

Unlike the piezoelectric constants e_{ij} , electromechanical coefficients d_{ij} are the response of strain to *nonzero* electric field, and its determination requires the handling of finite electric fields. This is challenging since infinite solids under finite electric fields do not possess a ground state,⁹ and the general approach of searching for the lowest energy configuration using density-functional theory (DFT) thus cannot be applied in a straightforward manner. Direct determination of d_{33} from first principles has been possible only recently.¹⁰⁻¹³ By constraining the polarization direction, Fu and Cohen calculated the electromechanical response of BaTiO₃ to a non-collinear electric field by using only the DFT total energy.¹⁰ Sai *et al.* developed a systematic theory of “constrained polarization approach” by which the atomic structure and cell shape—for a given constrained polarization (including both direction and magnitude)—are determined using density-functional linear response theory.¹¹ Souza *et al.* formulated a powerful “Bloch-theory approach” to determine both the electronic and ionic responses to finite electric fields by searching the metastable state of systems under finite electric fields.¹² More recently, Fu and Bellaiche presented a simple and efficient “constrained-force approach” for determining the ionic response of insulators to finite electric fields.¹³

Nevertheless, the electromechanical response in ZnO remains to be studied. First, determination of the d_{33} coefficient in wurtzite ZnO using accurate DFT theory has not been done before and is of its own value itself. Furthermore, little is known about how each individual atom may respond to finite electric fields, and how the atomic displacement couples with strain in wurtzite structure. Similarly, it is not clear why electric fields are able to introduce large mechanical response in ZnO, but not in other semiconductors. Another interesting question is whether it is possible to discover a general mechanism that governs the electromechanical re-

sponse in all tetrahedral semiconductors, in addition to ZnO alone. This mechanism, if it exists, ought to be useful and thus needed for guiding the design of new semiconductors with enhanced electromechanical responses.

It is worth pointing out that another and very active field of studying electromechanical response is, in fact, on ferroelectric and piezoelectric perovskite oxides.^{14,15} A theory of fundamental importance, namely the modern theory of polarization, has been spectacularly developed.^{16,17} Experimentally, single crystal $\text{Pb}(\text{MgNb})\text{O}_3\text{—PbTiO}_3$ (PMN-PT) and $\text{Pb}(\text{ZnNb})\text{O}_3\text{—PbTiO}_3$ (PZN-PT) solid solutions were found to exhibit an enormous piezoelectric response on the order of ~ 2500 pC/N, which is ten times greater than in traditional piezoelectric ceramics.¹⁸ This remarkable response has been explained by polarization rotation, in which the electric field—applied non-collinearly along the pseudocubic [001] direction rather than the rhombohedral [111] direction of spontaneous polarization—is able to cause the polarization to rotate with much less energy, thus leading to a large strain response.^{10,18} Despite the fact that a substantial amount of knowledge has existed in the field of ferroelectrics, there has been little connection between the understanding of the electromechanical responses in tetrahedral semiconductors and in ferroelectric perovskites. This connection, at the present stage, is of value in bridging these two fields.

The goals of this paper are (1) to determine the electromechanical response d_{33} in ZnO using a direct DFT theory and to understand what causes the large response in this particular semiconductor, and (2) to demonstrate that the two seemingly unrelated electromechanical responses in ZnO and in piezoelectric single crystals PMN-PT and PZN-PT have the same microscopic origin—namely, polarization rotation, thus connecting the studies of two different fields. However, unlike the case of ferroelectrics, electric fields in wurtzite semiconductors do not rotate the *total* net polarization; instead they rotate the *local* polarization of individual polar bonds. Based on our results, we also make some suggestions that we hope to be useful for the design of the electromechanical response in wurtzite semiconductors.

II. THEORETICAL METHODS

A. Structural optimization under finite electric fields

Our method that allows us to determine the cell shape and atomic positions for solids *under finite electric fields* was proposed and briefly described previously,¹³ based on the fact that electromechanical response arises predominantly from the ionic contribution. Here we give details of the method for two purposes: first, to provide computational techniques that may be useful for readers who are interested in its implementation and, second, to facilitate the discussions of our results on ZnO. To compute the electromechanical response in infinite solids, we determine, for a given finite electric field \mathcal{E} , the optimal strain $\{\eta_i\}$ (using Voigt notation) by searching for the minimum of free energy $F(\mathbf{R}, \eta, \mathcal{E}) = U_{\text{KS}}[\mathbf{R}(\mathcal{E}), \eta(\mathcal{E})] - P(\mathbf{R}, \eta, \mathcal{E}) \cdot \mathcal{E}$ as a function of strain. The Kohn-Sham internal energy U_{KS} and the macro-

scopic polarization \mathbf{P} both depend on the atomic positions $\{\mathbf{R}\}$ and the strain $\{\eta\}$, which are further implicitly dependent on the field \mathcal{E} . We should point out that \mathcal{E} in the expression of free energy is the screened macroscopic (not external) electric field. For a given field \mathcal{E} , we determine U_{KS} and \mathbf{P} for a series of chosen and prefixed strains $\{\eta\}$. For each strain, atomic positions are fully relaxed so that the free energy reaches its allowed subspace minimum under the specified strain. This requires the total force—including the normal Hellmann-Feynman (HF) force Q_{HF}^i arising from the first term of the free energy and the electrostatic force arising from the second term—to vanish. In other words, the HF force Q_{HF}^i on atom i should thus satisfy

$$Q_{\text{HF}}^i = -Z_i^*(\mathbf{R}, \eta, \mathcal{E})\mathcal{E}, \quad (1)$$

where Z_i^* is the Born effective charge tensor of ion i . Numerically, we search for the structure that satisfies the above force constraint by first computing the normal HF force Q_{HF}^i under zero field, which is then added to the electrostatic force due to the applied electric field. The total force is then minimized using the standard variable metric method of a Hessian matrix. This approach is hereafter referred to as the “force-constrained method.”

An alternative approach to determine the atomic geometry that satisfies Eq. (1) is, as similarly proposed in Ref. 11, to expand the HF force $Q_{\text{HF}}^i(\mathbf{R})$ at the *field-induced* position \mathbf{R} as a linear function of the atomic displacement, namely, $Q_{\text{HF}}^i(\mathbf{R}) = Q_{\text{HF}}^i(\mathbf{R}_0) + \mathbf{D}(\mathbf{R} - \mathbf{R}_0)$, where \mathbf{R}_0 is the zero-field equilibrium position and \mathbf{D} is the force-constant dynamic matrix. The new atomic position under nonzero field can thus be determined by a single step as $\mathbf{R} = \mathbf{R}_0 - \mathbf{D}^{-1}Z_i^*\mathcal{E}$. For ordinary materials such as semiconductors or *normal* ferroelectrics, we find that this approach generally is as convenient as the force-constrained method, provided that the force-constant matrix is available by means of, for instance, the density-functional linear response theory. On the other hand, we also find that, for *incipient* ferroelectrics such as SrTiO_3 in which a small electric field is able to drive very large atomic displacements (i.e., \mathbf{D} is near its singularity), the force-constant approach within the linear approximation yields qualitatively incorrect results, while the force-constrained method still works robust.¹⁹

With optimized atomic positions, we compute the internal energy U_{KS} and polarization as a function of strain, for a given electric field. For the purpose of determining d_{33} , we need to consider only the polarization component P along the field direction. At this stage, one may determine the optimal strain that yields the minimum free energy by *numerically* examining the free energy-versus-strain relationship. However, we find that this numerical scheme tends to produce large fluctuation and error. Instead, we fit the strain dependence of U_{KS} and P using analytical expressions $U_{\text{KS}}(\mathcal{E}, \eta_3) = U_0(\mathcal{E}) + \alpha\eta_3^2$ and $P(\mathcal{E}, \eta_3) = P_0(\mathcal{E}) + \beta\eta_3$, where U_0 and P_0 are the respective values of the energy and polarization at zero strain but under nonzero electric fields. These analytical forms not only are convenient for determining the minimum free energy, but also render transparent physical meaning. More specifically, the α parameter is related to the

elasticity of the material along the direction of the applied field, while the β parameter is the piezoelectric coefficient that describes the response of polarization to the strain. Minimizing the free energy with respect to the η_3 strain for a given electric field \mathcal{E} yields analytically

$$\eta_3 = \frac{\beta}{2\alpha} \mathcal{E}, \quad (2)$$

and the electromechanical d_{33} coefficient is thus $\beta/2\alpha$. Strictly speaking, the parameters α and β depend on the field strength \mathcal{E} . But we found that, over a wide range of field strengths, these two parameters are nearly independent of the applied field. Performing calculations for a single field strength can thus determine the coefficient d_{33} . We suggest that the field strength be chosen on the order of 0.02 V/\AA , since smaller fields may cause unnecessary numerical uncertainty.

B. Details of first-principles pseudopotential calculations

Total energy and atomic forces are calculated using our first-principles pseudopotential code with a mixed-basis set.²⁰ The local density approximation (LDA)²¹ is used to describe electron exchange-correlation interaction. Core electrons are replaced by orbital-dependent nonlocal pseudopotentials that are carefully generated following Troullier-Martins' scheme.²² We use ionic configuration $3d^{10}4s^14p^{0.1}$ and pseudo/all-electron wave-function radii of $r^{s,p,d}=2.0, 2.0,$ and 2.5 Bohr to generate Zn pseudopotentials. For oxygen atom, we use $2s^22p^43d^0$ and $r^{s,p}=1.5, 1.5$ Bohr to generate its s and p pseudopotentials, and $2s^22p^33d^{0.3}$ and $r^d=2.5$ Bohr for its d pseudopotential. The d pseudopotential of the O atom is generated separately because the d orbital in neutral or negatively charged ionic configuration is very extended, and this pseudopotential needs to be generated using a positively charged ionic configuration. The semi-core state of Zn $3d$ is treated explicitly as a valence electron to ensure accuracy. An energy cutoff of 884 eV (65 Ry) is used and is found to be sufficient for convergence. To calculate electric polarization, we have implemented the modern theory of polarization^{16,17} in our mixed-basis method using the geometric phase of valence wave functions.²⁰ Effective charges are calculated as the derivative of polarization with respect to atomic displacement via finite difference. For systems under electric field, atomic positions are relaxed until the total force on each atom is less than $5 \times 10^{-4} \text{ eV/\AA}$.

III. RESULTS AND DISCUSSIONS

Zero-field equilibrium structure and Born effective charge: Figure 1 shows schematically the crystal structure of wurtzite ZnO. Our LDA calculations yield for ZnO at zero field an equilibrium structure with an in-plane lattice constant $a=3.25 \text{ \AA}$, $c/a=1.62$, and a u parameter of 0.3781 (where c is the lattice constant along the polar axis, and u denotes the ratio between the Zn_1 - O_1 bond length and the c lattice constant). These results are in good agreement with the experimental values of $a=3.253 \text{ \AA}$, $c/a=1.60$, and $u=0.3820$.²³ The spontaneous polarization per unit cell in the

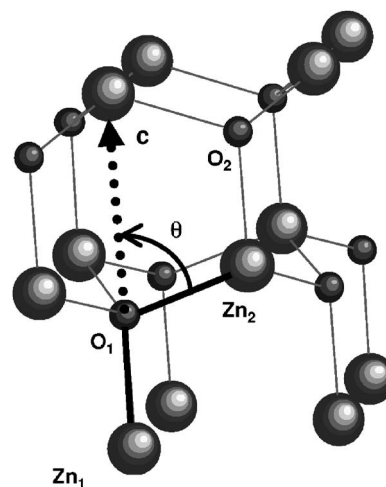


FIG. 1. Crystal structure of wurtzite ZnO, with individual Zn_1 , Zn_2 , O_1 , and O_2 atoms and the c axis labeled. Angle θ is between the Zn_2 - O_1 bond and the c axis.

LDA-predicted ZnO structure is determined to be $2.548 \text{ e} \cdot \text{\AA}$. The effective charges of Zn and O are calculated to be 2.20 and -2.20 , compared to the experimental value of 2.10 (Ref. 24) and other theoretical values of 2.05 (Ref. 7, obtained from LAPW method) and 2.07 (Ref. 8, obtained from plane-wave pseudopotential method). We thus see that, unlike in ferroelectric titanate perovskites, the effective charges in semiconductor ZnO are close to the nominal values and do not reveal any anomaly.

Determination of electromechanical coefficient d_{33} : Figure 2 shows the internal Kohn-Sham energy as a function of the η_3 strain for ZnO under an electric field of 0.02 V/\AA that is applied along the c axis. Here we find that a sufficient energy cutoff is particularly important for obtaining a quantitatively accurate description of the small-scale energy variation in Fig. 2. To ensure the accuracy of our calculations, we also present in Fig. 2 the results of a larger energy cutoff (i.e., 984 eV) for comparison, showing that two calculations yield the same curvature (and thus the same α parameter). Analytically fitting our calculated internal energy U_{KS} produces an α parameter of 31.66 eV .

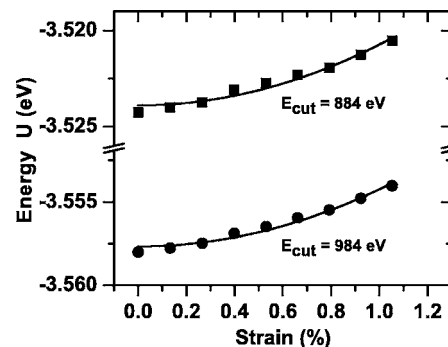


FIG. 2. Internal energy U_{KS} (relative to an energy base of -3680 eV) as a function of the η_3 strain in ZnO under a finite electric field of 0.02 V \AA^{-1} . Symbols are direct DFT calculation results, and curves are analytical fitting. Results obtained using two different cutoff energies are shown for comparison.

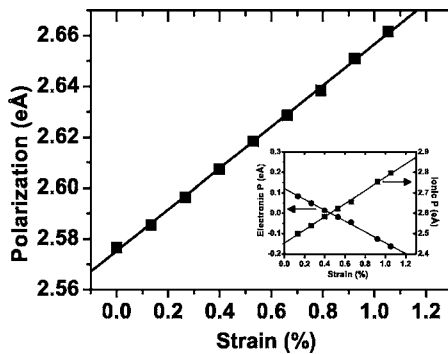


FIG. 3. Total polarization as a function of the η_3 strain in ZnO under an electric field of 0.02 V \AA^{-1} . The inset shows the electronic and ionic contributions to the total polarization.

Figure 3 depicts the polarization as a function of the η_3 strain, showing a linear dependence up to a strain of 1.2%, which is the largest strain we consider. It should be pointed out that, for each strain, the atomic geometry is fully relaxed and recalculated, and so is the polarization. The perfect linear dependence produced by the direct DFT calculations is thus not trivial as it may appear to be; it indicates that our method of structural optimization under finite electric fields indeed is robust. The polarization-strain slope (i.e., the β parameter) is determined to be 8.13 e\AA . We further decompose the polarization into ionic and electronic contributions, as shown in the inset of Fig. 3. The ionic contribution is found to increase with the increasing strain, whereas the electronic contribution shows the opposite trend. The polarization-vs.-strain slope of the ionic contribution turns out to be larger than that of the electronic contribution, giving rise to a net increase of the polarization as the strain increases.

Using Eq. (2) and the above α and β values obtained from our direct first-principles calculations, the electromechanical coefficient d_{33} is determined to be 12.84 pC/N . This value is in excellent agreement with the experimental value of 12.4 pC/N . This level of agreement is obtained without adjustable inputs from experiments, demonstrating that the first-principles DFT method under finite electric fields is able to predict reliably the electromechanical properties.

Comparison with GaN and PbTiO₃: One appealing aspect of the analytical expression in Eq. (2) is its physical transparency, revealing that a large electromechanical response arises from either a small elasticity of the material (i.e., small α) or a large polarization response to strain (i.e., large β). It is interesting to compare the α and β quantities of ZnO with those of GaN, which is also a semiconductor with the same wurtzite structure—and with those of PbTiO₃, which is a ferroelectric with large electromechanical response. For GaN, the α and β values are 67.14 eV and 2.12 e\AA , respectively, while for PbTiO₃ they are 4.36 eV and 11.22 e\AA (Ref. 13). These yield a d_{33} value of 1.58 pC/N for GaN and 128.8 pC/N for PbTiO₃.

Comparison between ZnO and GaN shows that the large d_{33} response in ZnO is mainly due to its large polarization response to the imposed strain, i.e., large β value. More specifically, this value is about four times greater in ZnO than in

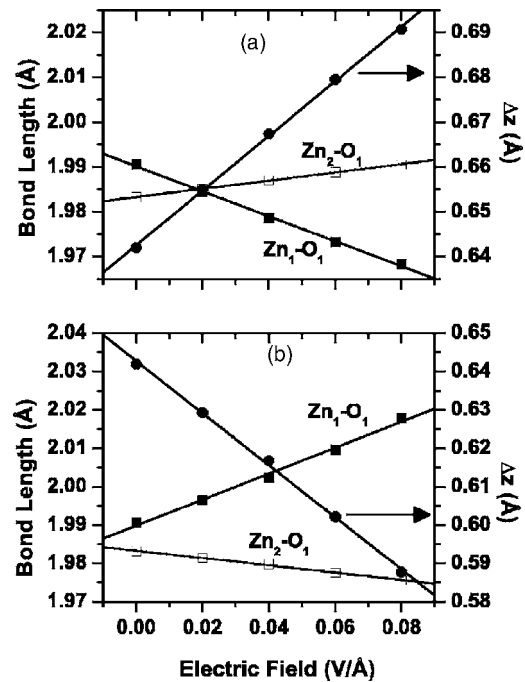


FIG. 4. Bond lengths of $\text{Zn}_1\text{-O}_1$ (filled squares, using the left vertical axis) and $\text{Zn}_2\text{-O}_1$ (empty squares, using the left vertical axis), and the projected length ΔZ of the $\text{Zn}_2\text{-O}_1$ bond along the c axis (filled dots, using the right vertical axis) as a function of field magnitude: (a) for positive fields applied along the c axis and (b) for negative fields applied opposite to the c axis.

GaN. It should be pointed out that this difference cannot be explained by the effective charge. In fact, the effective charge of ZnO (for which the LDA value is 2.20) is smaller than the corresponding LDA value of 2.77 for GaN. Instead, the strong coupling between strain and atomic displacements is the reason for the large β value in ZnO. The relatively smaller α parameter in ZnO than in GaN also contributes to the difference in their d_{33} coefficients. Our calculated α values (31.66 eV in ZnO versus 67.14 eV in GaN) tell that ZnO is more deformable along the polar c axis. This result is consistent with the fact that the elastic C_{33} constant for ZnO (2.1 Mbar , Ref. 25) is about half of the value for GaN ($\sim 4.1 \text{ Mbar}$, Ref. 26). The contrast between ZnO and PbTiO₃ shows that the exceptionally small α of lead titanate—in other words, the very flat energy surface—is the main cause for the drastic difference in electromechanical response between ferroelectrics and semiconductors.

Microscopic mechanism for electromechanical response in wurtzite semiconductors. To provide microscopic insight as to how individual atoms in ZnO respond to electric fields, we perform structural optimization under different field strengths and decide to examine the lengths b for nonequivalent $\text{Zn}_1\text{-O}_1$ and $\text{Zn}_2\text{-O}_1$ bonds as well as the projected length $\Delta Z \equiv b(\text{Zn}_2\text{O}_1)\cos\theta$ of the second bond along the c axis. Note that ΔZ characterizes the effect of the $\text{Zn}_2\text{-O}_1$ bond on altering the c axis strain (see Fig. 1). The results are depicted in Fig. 4(a) for electric fields applied along the polarization direction (abbreviated as positive fields hereafter) and in Fig. 4(b) for electric fields applied opposite to the polarization direction (abbreviated as negative fields). The

branch of the spontaneous polarization is chosen in our calculations to be along the positive c axis of Fig. 1.

It has been commonly thought that the stretching or compression of the $\text{Zn}_1\text{-O}_1$ bond that points collinearly with the polar axis of wurtzite structure is the main force for driving the c -axis length as a result of the coupling between atomic displacement and strain. Our calculations, however, reveal otherwise. Under the positive fields [Fig. 4(a)], the $\text{Zn}_1\text{-O}_1$ bond indeed (and not surprisingly) is found to be compressed, with a slope of field-induced length change determined to be $0.278 \text{ \AA}^2/\text{V}$. Interestingly, the $\text{Zn}_2\text{-O}_1$ length is predicted to remain nearly constant as the field strength increases. However, its projected length ΔZ is found to increase sharply. The slope of the ΔZ curve is found to be $0.610 \text{ \AA}^2/\text{V}$, which is more than two times larger than that of the $\text{Zn}_1\text{-O}_1$ curve. These results thus demonstrate an important conclusion, namely that the dominant effect of the electric fields in wurtzite semiconductors is not to elongate the polar chemical bonds, but to rotate those bonds that are *non-collinear* with the polar c axis towards the direction of the applied electric fields. A similar conclusion is also true for the negative fields that are found in our calculations to drastically decrease the projected length ΔZ as compared to the slight increase of the $\text{Zn}_1\text{-O}_1$ length, as shown in Fig. 4(b). Once again, the length of the noncollinear $\text{Zn}_2\text{-O}_1$ bond is nearly unchanged.

According to the above observations, the electromechanical response in wurtzite semiconductors becomes interestingly similar to the polarization rotation mechanism as previously found in ferroelectric and piezoelectric single crystals.^{18,10,27,28} In the latter case, the polarization rotation was shown to lead to much enhanced electromechanical response, as compared to the collinear fields that are applied along the direction of spontaneous polarization.^{18,28} In both circumstances, polarization rotation occurs because less energy is needed to alter the direction of polarization than to enlarge its magnitude. However, there is a difference: unlike the case of ferroelectric perovskites where the electric field rotates the total polarization as a whole, the electric field in

wurtzite crystals rotates “only” the chemical bonds (in a loose sense, the local polarization) while the total polarization always points along the c axis.

Revealing the bond rotation mechanism in wurtzite structure also provides useful knowledge on how electromechanical response in semiconductors can be improved. We note that the energy for rotating the noncollinear bonds in wurtzite semiconductors is largely used for overcoming the bond bending by reducing the related bond angles. Efficient semi-conducting actuators with better electromechanical response should thus have smaller bond bending energy to facilitate the bond rotation. The bond-bending distortion energy, which is described by, for instance, the Keating model,²⁹ can thus be a useful quantity to guide the design of the electromechanical performance in semiconductors. Our future work will be to systematically compute the electromechanical response and bond bending energy in different wurtzite semiconductors and to establish a quantitative correlation between these quantities.

In summary, we have determined the electromechanical coefficient in wurtzite zinc oxide using a direct first-principles density functional approach under finite electric fields. Our theoretical d_{33} value of 12.84 pC/N is in good agreement with the experimental measurement. We further found that the dominant effect of electric fields in wurtzite semiconductors is to rotate the noncollinear polar bonds towards the c axis, which consequently drives the strain. The microscopic mechanism for governing the electromechanical response in wurtzite semiconductors is thus rather similar to the polarization rotation in piezoelectric single crystals PZN-PT and PMN-PT. In addition, comparison of the electromechanical responses of ZnO, GaN, and PbTiO_3 reveals that the main difference between ZnO and GaN is characterized by the piezoelectric polarization-vs.-strain response, and the difference between wurtzite semiconductors and ferroelectric perovskites lies in the energy-strain surface.

We thank I. Naumov and L. Bellaiche for discussions. This work was supported by NSF (DMR-0116315) and ONR (N00014-01-1-0366).

¹Z. W. Pan, Z. R. Dai, and Z. L. Wang, *Science* **291**, 1947 (2001).

²M. C. Tamargo, ed., *II-VI Semiconductor Materials and Their Applications* (Taylor & Francis, New York, 2002).

³V. Ranjan, L. Bellaiche, and E. J. Walter, *Phys. Rev. Lett.* **90**, 257602 (2003).

⁴A. Wander, F. Schedin, P. Steadman, A. Norris, R. McGrath, T. S. Turner, G. Thornton, and N. M. Harrison, *Phys. Rev. Lett.* **86**, 3811 (2001).

⁵O. Dulub, U. Diebold, and G. Kresse, *Phys. Rev. Lett.* **90**, 016102 (2003).

⁶S. Limpjumnong, S. B. Zhang, S.-H. Wei, and C. H. Park, *Phys. Rev. Lett.* **92**, 155504 (2004).

⁷A. Dal Corso, M. Posternak, R. Resta, and A. Baldereschi, *Phys. Rev. B* **50**, 10715 (1994).

⁸N. A. Hill and U. Waghmare, *Phys. Rev. B* **62**, 8802 (2000).

⁹R. W. Nunes and D. Vanderbilt, *Phys. Rev. Lett.* **73**, 712 (1994).

¹⁰H. Fu and R. E. Cohen, *Nature (London)* **403**, 281 (2000).

¹¹N. Sai, K. M. Rabe, and D. Vanderbilt, *Phys. Rev. B* **66**, 104108 (2002).

¹²I. Souza, J. Iniguez, and D. Vanderbilt, *Phys. Rev. Lett.* **89**, 117602 (2002).

¹³H. Fu and L. Bellaiche, *Phys. Rev. Lett.* **91**, 057601 (2003).

¹⁴M. E. Lines and A. M. Glass, *Principles and Applications of Ferroelectrics and Related Materials* (Clarendon, Oxford, 1979).

¹⁵R. E. Cohen, *Nature (London)* **358**, 136 (1992).

¹⁶R. D. King-Smith and D. Vanderbilt, *Phys. Rev. B* **47**, R1651 (1993).

¹⁷R. Resta, *Rev. Mod. Phys.* **66**, 899 (1994).

¹⁸S.-E. Park and T. R. Shrout, *J. Appl. Phys.* **82**, 1804 (1997).

¹⁹I. Naumov and H. Fu, Preprint at cond-mat/0409330 (2004).

²⁰H. Fu and O. Gulseren, *Phys. Rev. B* **66**, 214114 (2002).

- ²¹W. Kohn and L. J. Sham, Phys. Rev. **140**, A1133 (1965).
- ²²N. Troullier and J. L. Martins, Phys. Rev. B **43**, 1993 (1993).
- ²³H. Schulz and K. H. Thiemann, Solid State Commun. **32**, 783 (1979).
- ²⁴*Elastic, Piezoelectric, Pyroelectric Constants and Nonlinear Dielectric Susceptibilities of Crystals*, Landolt-Bornstein New Series, Group III, Vol. 11 (Springer, Berlin, 1979).
- ²⁵T. B. Bateman, J. Appl. Phys. **33**, 3309 (2005).
- ²⁶J.-M. Wagner and F. Bechstedt, Phys. Rev. B **66**, 115202 (2002), and references therein.
- ²⁷A. Garcia and D. Vanderbilt, Appl. Phys. Lett. **72**, 2981 (1998).
- ²⁸H. Fu and R. E. Cohen, in *Fundamental Physics of Ferroelectrics*, edited by R. E. Cohen (AIP, New York, 2000), p 143.
- ²⁹R. M. Martin, Phys. Rev. B **1**, 4005 (1970).